Highly Transparent Low Resistance ZnO/Ag Nanowire/ZnO Composite Electrode for Thin Film Solar Cells

Areum Kim,[†] Yulim Won,[†] Kyoohee Woo,[†] Chul-Hong Kim,[‡] and Jooho Moon[†,*]

[†]Department of Materials Science and Engineering, Yonsei University, 50 Yonsei-ro, Seodaemun-gu, Seoul 120-749, Republic of Korea and [‡]R&D Center, LG Display Co., Ltd., Paju 413-811, Republic of Korea

ABSTRACT We present an indium-free transparent conducting composite electrode composed of silver nanowires (AgNWs) and ZnO bilayers. The AgNWs form a random percolating network embedded between the ZnO layers. The unique structural features of our ZnO/AgNW/ZnO multilayered composite allow for a novel transparent conducting electrode with unprecedented excellent thermal stability (~375 °C), adhesiveness, and flexibility as well as high electrical conductivity (~8.0 Ω/sq) and good optical transparency (>91% at 550 nm). Cu(In,Ga)(S,Se)$_2$ (CIGSSe) thin film solar cells incorporating this composite electrode exhibited a 20% increase of the power conversion efficiency compared to a conventional sputtered indium tin oxide-based CIGSSe solar cell. The ZnO/AgNW/ZnO composite structure enables effective light transmission and current collection as well as a reduced leakage current, all of which lead to better cell performance.

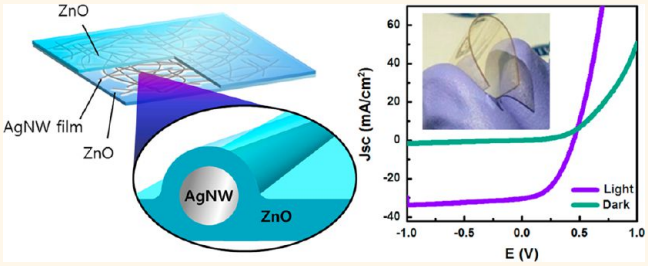

KEYWORDS: indium-free transparent electrode · silver nanowire · zinc oxide · multilayer composite electrode · thin film solar cells

The need for highly transparent electrodes with a low resistance has become more significant not only for flat-panel display (FPD) and touch-panel screen industries, which currently have a large market, but also for solar cell applications.[1] Solar panels are generally installed on rooftops or the ground, and therefore, they involve much larger transparent electrodes than those used for FPDs and touch-panel screens. Moreover, in general, solar cell applications require a relatively thick transparent electrode film about several hundred nanometers thick, while films with a thickness of several tens of nanometers are needed for display applications.[2] As a result, solar cell applications demand higher amounts of transparent electrode material than other electronic applications. To fabricate cost-effective solar cells, it is imperative to develop a low-cost transparent electrode with low resistivity and high transparency.

Although crystalline indium tin oxide (ITO) has been widely adopted as a transparent electrode in solar cells, it is an undesirable material for use in low-cost solar cells because of the scarcity of indium and its high deposition cost. Thus, various indium-free transparent electrode materials, such as metal nanowire networks,[3−11] conducting polymers,[12,13] carbon nanotubes,[14−16] graphene,[17−19] and several conducting oxides (Ga:ZnO,[20] Al:ZnO,[21] and In:ZnO[22]), have been extensively investigated as alternatives to ITO. Among these, silver nanowire (AgNW) films have recently attracted substantial interest as a transparent conducting material. Transparent electrodes composed of random AgNW networks can be readily achieved by simple and scalable solution processing such as spin coating,[6] rod coating,[11] drop casting,[3,4] and air spraying[7,23] from a AgNW dispersion. The AgNW network film fabricated at 140 °C is a promising electrode material for solar cells because of its low sheet resistance (~9.7 Ω/sq) and high transmittance (~89% at 550 nm).[6] Although there are previous reports demonstrating the AgNW exploitation in organic solar cells,[24] its utilization for thin film solar cells faces some problems. The environment surrounding the solar cells is harsh for AgNW films when used as a top transparent electrode that can be subjected to direct exposure to air and large temperature

* Address correspondence to jmoon@yonsei.ac.kr.

Received for review August 29, 2012 and accepted January 20, 2013.

Published online January 21, 2013
10.1021/nn305491x

increases (~200 °C). The AgNW film would undergo local oxidation and melting, which adversely affects the conductivity of the AgNW film. Although the melting point of bulk silver is above 960 °C, it can be depressed due to the high surface-to-volume ratio of the nanowires. It has been reported that annealing even at 200 °C could lead to an abrupt increase in the sheet resistance as the nanowires coalesce into isolated droplet-shaped Ag particles and the metallic phase network is disconnected.[4] In addition, the low carrier collecting efficiency of AgNW films could pose another hurdle. The limited contact area of AgNWs with n-type or buffer layers is incapable of effectively collecting the charge carrier generated at the p−n junction.

Recently, ZnO has also drawn significant attention as an alternative transparent conducting oxide because of its nontoxicity, low cost, and material abundance. However, the resistance of ZnO is too high for it to be used as a conducting electrode material. To increase its conductivity, ZnO is doped with impurities that act as an n-type dopant to release the free electron carrier. Another approach is to use ZnO/Ag thin film/ZnO multilayer sandwich-like structures such as those shown in Scheme 1a.[25−27] The insertion of an ultrathin silver film with the lowest resistivity (1.6×10^{-6} Ω·cm) can dramatically lower the sheet resistance, while the thin film at the nanometer scale can transmit visible light.[26] Han *et al.* reported a ZnO/Ag film/ZnO multilayer electrode with a low sheet resistance of 6 Ω/sq when a 12 nm thick Ag layer was utilized.[28] An ultrathin metal film can be replaced by a patterned film or metal grid to maintain a high electrical conductivity and to enhance the optical transparency, as shown in Scheme 1b.[29] Patterning of the metal layer can be accomplished by either electron beam lithography of the vacuum-deposited film or printing of conductive ink.[29] However, the patterning adds an additional process step, which makes the process more complicated and increases the production cost.

Here, we propose a similar layered structure of ZnO/AgNW/ZnO (Scheme 1c) to resolve the issues regarding the sole use of AgNWs and ZnO/Ag thin film (or grid)/ZnO composites. The AgNW network film contains inherent open spaces so that it can be considered as a natural random grid-like pattern at the several tens of nanometers scale. Incident light passes through the open areas in the ZnO/AgNW/ZnO multilayer, while it has to travel through the Ag thin film in the ZnO/Ag film/ZnO multilayer. The Ag film needs to be not only thin enough to be transparent but also thick enough to maintain the film conductance. By contrast, the well-connecting percolating network of Ag nanowires with a high aspect ratio ensures a high conductivity. The AgNW density plays an important role in determining the film conductivity and optical transparency, which can be readily controlled by either the concentration of the AgNW dispersion or the coating process.

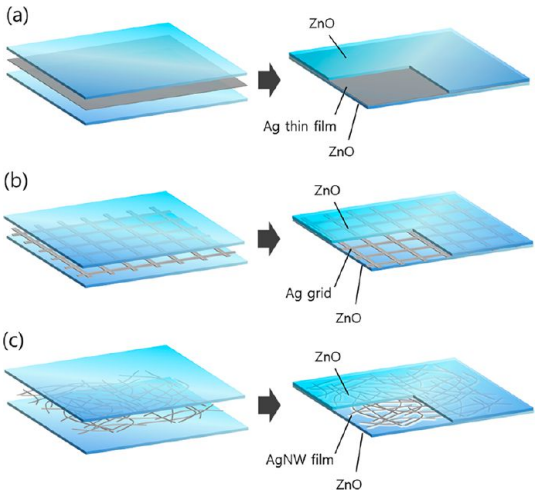

Scheme 1. Schematics of the conventional ZnO-based multilayer transparent electrode structure as well as the proposed multilayer transparent electrode structure. (a) ZnO/Ag film/ZnO structure with a Ag thin film layer between two transparent ZnO layers. (b) ZnO/Ag grid/ZnO structure in which the Ag grid is inserted. (c) ZnO/AgNW/ZnO structure in which a Ag nanowire network is present instead of a Ag thin film.

Furthermore, outer layers of ZnO embedding AgNWs in the sandwich structure could prevent the AgNWs from local melting-induced disconnection at the cross junctions, resulting in enhanced thermal stability of the AgNWs and improved adhesion of AgNWs to the substrate. Such a composite electrode is also capable of effective charge carrier collection due to filling the empty space unoccupied by AgNWs with ZnO materials as well as resulting in a better surface smoothness. Stubhan *et al.*[30] reported an indium-free bilayered composite electrode (AZO or ZnO/AgNW) as a cathode in organic thin film solar cells with an emphasis on the surface flattening effect; however, the enhancement of thermal and mechanical stabilities as well as the detailed optical and electrical properties were not clearly discussed.

In this work, we fabricated an indium-free ZnO/AgNW/ZnO composite electrode for thin film solar cells using spin-coated AgNW films and sputtered ZnO thin films. The electrical, optical, structural, mechanical, and thermal properties of the indium-free ZnO/AgNW/ZnO electrode were investigated as a function of the occupied density of the Ag network. Thanks to the low resistance and anti-reflection effect resulting from the inserted AgNWs, the $Cu(In,Ga)(S,Se)_2$ (CIGSSe) thin film solar cell using the ZnO/AgNW/ZnO top electrode exhibited a higher power conversion efficiency (PCE) than the reference CIGSSe cell based on a conventional sputtered ITO electrode.

RESULTS AND DISCUSSION

The ZnO/AgNW/ZnO composite electrodes were fabricated by inserting a AgNW film between two sputtered ZnO layers. The properties of the ZnO/AgNW/ZnO structure, including the sheet resistance

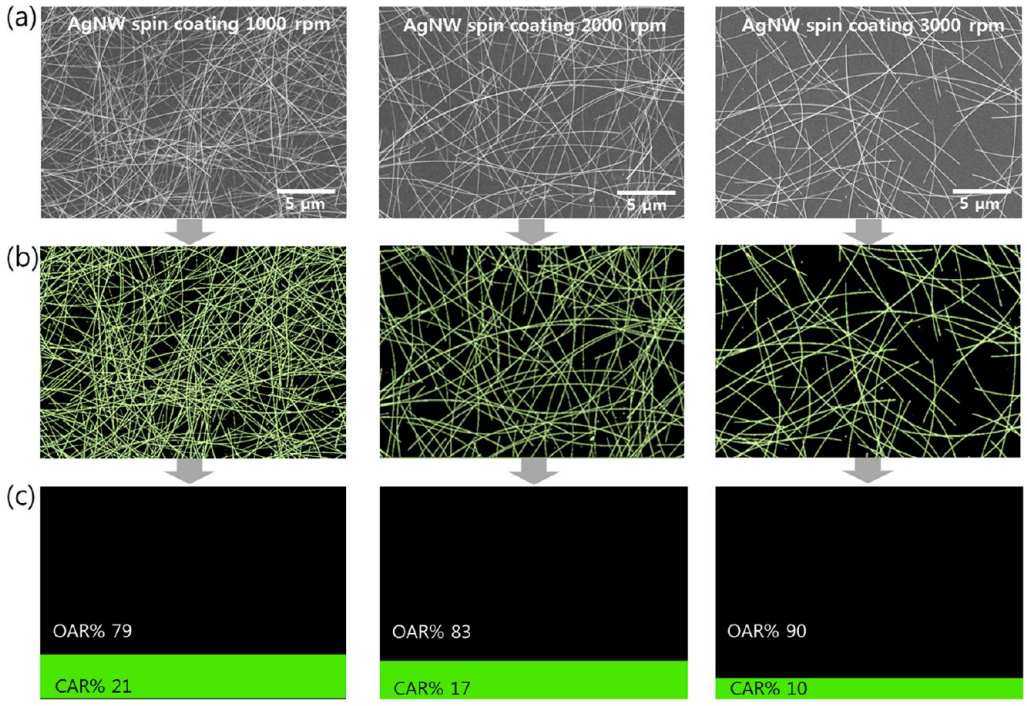

Figure 1. (a) SEM images of the AgNW/ZnO bilayer structure. The AgNW layers were prepared by spin coating at rotation speeds of 1000, 2000, and 3000 rpm. (b) Converted images showing the projected two-dimensional morphology of the composite. (c) Corresponding images showing the area fraction of the open area ratio (OAR) to the covered area ratio (CAR).

(R_s) and transmittance, have a close relationship with the AgNW density. When AgNW films are deposited by spin coating from a AgNW dispersion (Cambrios Technologies Corp.) at a given concentration, the NW density can be controlled by adjusting the rotation speed. A lower spin speed produces denser AgNW films. However, nanowire films with various densities cannot be characterized by simply the spin speed. Instead, the NW density is expressed in terms of the area coverage. The covered area ratio (CAR) represents the fraction of the area occupied by the AgNWs, whereas the open area ratio (OAR) indicates the unoccupied fraction. Figure 1 shows the conversion process used to obtain the CAR and OAR values. From the SEM images of the AgNW films spin coated at different spin speeds on ZnO/glass substrates, the OAR and CAR were determined by image analysis. Since the covered region counts the projected area on the two-dimensional plane as occupied by the AgNW, the overlapped area at the nanowire junctions or nanowire stacks are likely ignored. Although the CAR does not directly represent the NW density accurately, it serves as a simple descriptor to characterize the optical and electrical properties of the AgNW films.

Figure 2a shows the structure of the ZnO/AgNW/ZnO composite electrode along with its optical and electrical characteristics. The high-resolution transmission electron microscopy (HRTEM) cross-sectional image revealed that the ZnO/AgNW/ZnO sandwich structure is asymmetric. The bottom ZnO layer was flat with a thickness of ~32 nm, while the 33 nm thick top ZnO layer conformally coated the protruding AgNWs, as depicted in the schematic of Figure 2a (left).

Additional analysis of the surface morphology of the ZnO/AgNW/ZnO composite film was performed by atomic force microscopy (AFM) (Supporting Information, Figure S1). The AgNW diameter became larger compared to the diameter in the AgNW single layer due to the ZnO overcoat. The microstructural analyses confirmed that AgNWs are fully embedded between the ZnO layers, and a ZnO layer fills the empty spaces between the AgNW networks, making the surface of the AgNW film smoother. As shown in Figure 2c,d, the optical transmittance and reflectance of the ZnO/AgNW/ZnO electrodes on the glass substrates were measured as a function of the CAR. All of the composite electrodes are transparent so that our University logo is clearly visible through the electrodes (Figure 2b). Except for the sample with a CAR of 32%, all of the ZnO/AgNW/ZnO composite electrodes (CAR = 10−27%) showed higher transmittances than the ZnO double layered film (CAR = 0%) in the visible light region (450−800 nm).

This phenomenon can be explained by the antireflection effect due to an inserted AgNW layer suggested by Fan *et al.*[31] It was confirmed by the reflectance measurement that the reflectance in the ZnO/AgNW/ZnO composite is decreased when a AgNW layer is introduced (Figure 2d). All samples (CAR = 10−27%) exhibited a lower reflectance in the visible

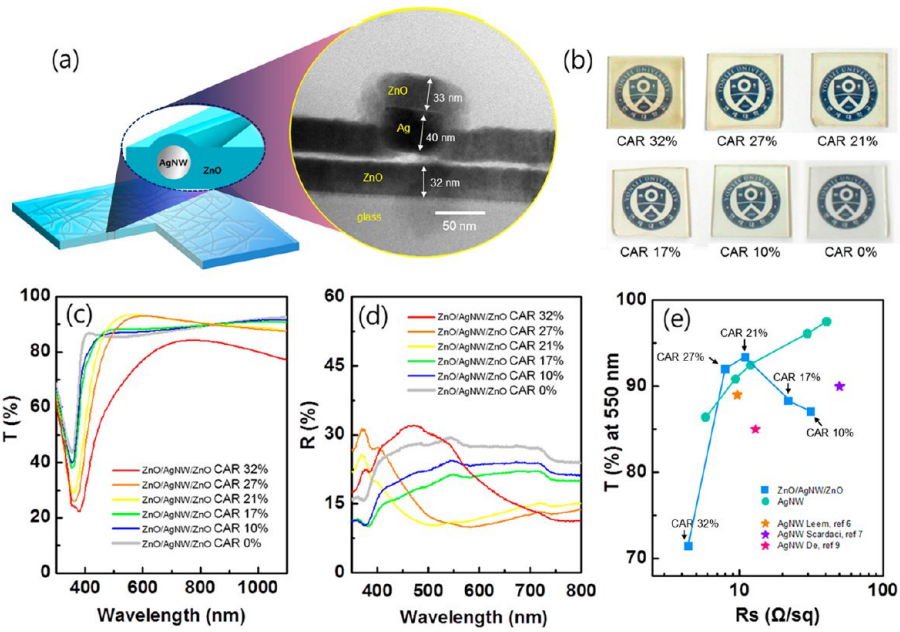

Figure 2. (a) Schematic structure of the ZnO/AgNW/ZnO composite electrode and a HRTEM cross-sectional image. (b) Photographs showing the ZnO/AgNW/ZnO composite electrodes with the various CAR values. (c) Optical transmittance and (d) reflectance of ZnO/AgNW/ZnO composite electrodes with the various CAR values. (e) Plot of transmittance (at λ = 550 nm) *versus* sheet resistance for the films of AgNWs (green circle) and ZnO/AgNW/ZnO (blue square). The points marked by stars represent the best results reported in the literature.[6,7,9]

light region than the ZnO double layer except for the sample with a CAR of 32%. At a wavelength of 550 nm, the reflectance of the ZnO film (CAR = 0%) was 29.16%, while the reflectance values of the ZnO/AgNW/ZnO with CAR values of 27 and 22% were 10.51 and 10.99%, respectively. The discrepancy of the sample with a CAR of 32% can be attributed to reflecting and scattering light by the AgNWs. This sample contains a relatively high AgNW density so that the dense and thick AgNW film can act like a mirror. This result indicates that control of the AgNW density is an important factor to maximize the optical properties of ZnO/AgNW/ZnO when used as a top window electrode.

Figure 2e shows the plots of the measured transmittance at λ = 550 nm *versus* R_s for AgNW film and ZnO/AgNW/ZnO composite. The film of ZnO/AgNW/ZnO with a R_s of 8.0 Ω/sq transmitted 91.91% light, while the film of the AgNW with a R_s of 9.4 Ω/sq allowed 90.81% light transmission. Some of the outstanding results reported in the literature for AgNW transparent conductors[6,7,9] are marked in Figure 2e. Our best results of the ZnO/AgNW/ZnO (CAR = 21−27%) composite electrode are comparable to the state-of-the-art AgNW transparent electrodes. However, in the low CAR region (CAR = 10−17%), the ZnO/AgNW/ZnO composite showed lower transmittance than the AgNW film due to significant absorption and reflection, indicating that the ZnO/AgNW/ZnO composite had an optimum CAR range.

For solar cell applications, the transparent electrode layer should have a low sheet resistance and allow transmission of most of the incident light to the absorber layer.[32] To determine the optimum CAR of the AgNWs in the ZnO/AgNW/ZnO composite electrode, the sheet resistance (R_s) and transmittance (T) at a wavelength of 550 nm were used to calculate the figure of merit Φ_{TC}, as defined by Haacke.[33]

$$\Phi_{TC} = \frac{T^{10}}{R_s}$$

Figure 3 exhibits the calculated Φ_{TC} as a function of the CAR. The Φ_{TC} values increase with increasing CAR up to 27%. The maximum Φ_{TC} value of 54 × 10^{-3} Ω^{-1} was obtained in the CAR = 27% sample (T = 91.91% and R_s = 8.0 Ω/sq). Although the composite electrode with a higher AgNW density (*i.e.*, CAR higher than 27%) exhibited a lower sheet resistance, we were unable to increase the AgNW density beyond a critical value due to severe loss of the optical transparency, which leads to a significant decrease of the Φ_{TC} value. As a result, the ZnO/AgNW/ZnO composite electrode with a CAR of 27% allows more light transmission at the visible wavelengths, while maintaining a high electrical conductance. As a result, the ZnO/AgNW/ZnO composites with a CAR of 27% showing the highest value of figure of merit were adopted as a transparent electrode in the thin film solar cells.

Table 1 summarizes the sheet resistance, transmittance, and figure of merit of the optimized ZnO/AgNW/ZnO composite electrode (CAR = 27%) with respect to the sputtered ITO film, the solution-processed AgNW film (CAR = 27%), and the sputtered ZnO films without insertion of a AgNW layer. The ZnO film exhibited a sheet resistance of about 136 kΩ/sq, which is too high to be applied as an electrode layer for solar cells. On the

other hand, the sheet resistance of the ZnO/AgNW/ZnO composite electrode dramatically decreased to 8.0 Ω/sq when the AgNW film was inserted. Although the AgNW film has the same CAR as the ZnO/AgNW/ZnO composite, the sheet resistance of the composite electrode is lower than AgNW single layer (Supporting Information, Figure S2). This phenomenon can be explained by the role of the ZnO layer to enhance the conductance of the AgNW film in the ZnO/AgNW/ZnO composite electrode. The overlying ZnO layer could decrease the sheet resistance by filling the voids between AgNWs and/or tightening the AgNW junction contact.[34,35] In addition, the ZnO layer could act as encapsulates, protecting the nanowires from oxidation or melting and, in turn, improve the mechanical and thermal stabilities of the AgNW film.[36,37]

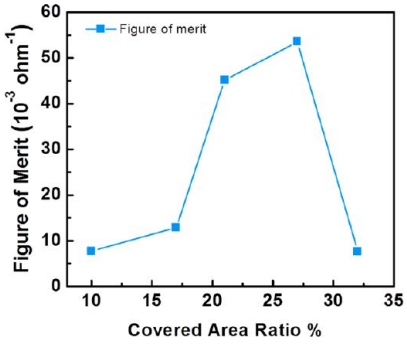

Figure 3. Figure of merit values of the ZnO/AgNW/ZnO electrodes as a function of the CAR in the range of 10−32%.

Metallic nanowire networks are recognized as a promising flexible electrode due to their outstanding bending properties.[9−11] To satisfy the mechanical requirements as a promising alternative candidate to conventional ITO electrodes, the transparent ZnO/AgNW/ZnO composite electrode should have better flexibility than the ITO film which is prone to cracking.[38] To compare the flexibility of the ZnO/AgNW/ZnO film to the ITO film, the bending test was performed in which the films were repeatedly bent at a radius of curvature of 3 mm (Figure 4a, bottom). Figure 4a (top) shows a photograph of the ZnO/AgNW/ZnO film on a polyethersulfone (PES) substrate, demonstrating its flexibility and transparency. The resistance variations obtained during the repetitive bending is represented by the $R_{s(n)}/R_{s(o)}$ ratio, where $R_{s(o)}$ is the initial sheet resistance and $R_{s(n)}$ is the sheet resistance measured when flattened after a certain number of bending cycles (Figure 4b). The ZnO/AgNW/ZnO composite electrode maintained a nearly similar resistance even after 500 bending cycles, while the sheet resistance of the ITO film soared after 50 cycles. It is notable that the ZnO/AgNW/ZnO composite electrode shows a very high tolerance to bending stress compared to the ITO film, and this mechanical stability strengthens the merit of the composite electrode with its low resistance and high transparency, which are comparable to ITO.

Although AgNW network films demonstrated higher conductivities and outstanding flexibilities compared to the ITO films, their application to solar cells poses

TABLE 1. Comparison of the Electrical and Optical Properties of Sputtered ITO at 100 °C, Sputtered ZnO (CAR = 0%) at 100 °C, AgNW Film (CAR = 27%) at 140 °C, and ZnO/AgNW/ZnO Composite Film (CAR = 27%)

	sheet resistance (Ω/sq)	transmittance (%) at 550 nm	figure of merit (10^{-3} Ω^{-1})
sputtered ITO (100 °C)	42	90.57	8.8
sputtered ZnO (100 °C)	135,950	82.69	1.1×10^{-3}
AgNW (CAR = 27%)	9.4	90.81	41
ZnO/AgNW/ZnO (CAR = 27%)	8.0	91.91	54

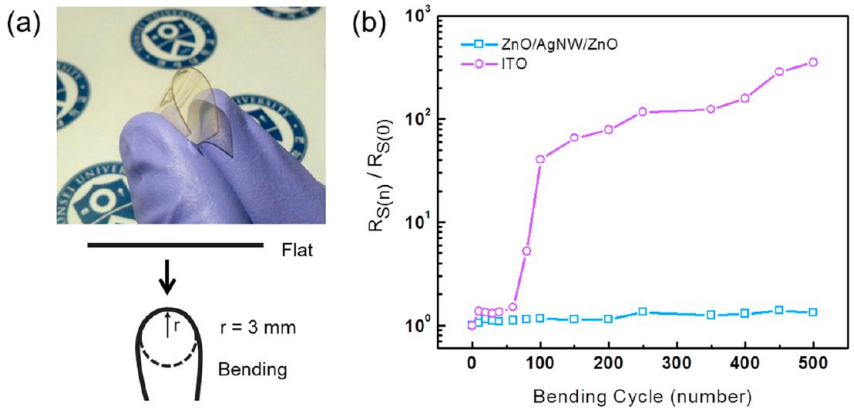

Figure 4. (a) Photograph of a flexible and transparent ZnO/AgNW/ZnO composite electrode on a flexible polymer substrate (top) and schematics showing the mechanical bend test conditions (bottom). (b) Changes of the normalized resistance during the bend test for the sputtered ITO single layer and the ZnO/AgNW/ZnO composite layer on polymer substrates.

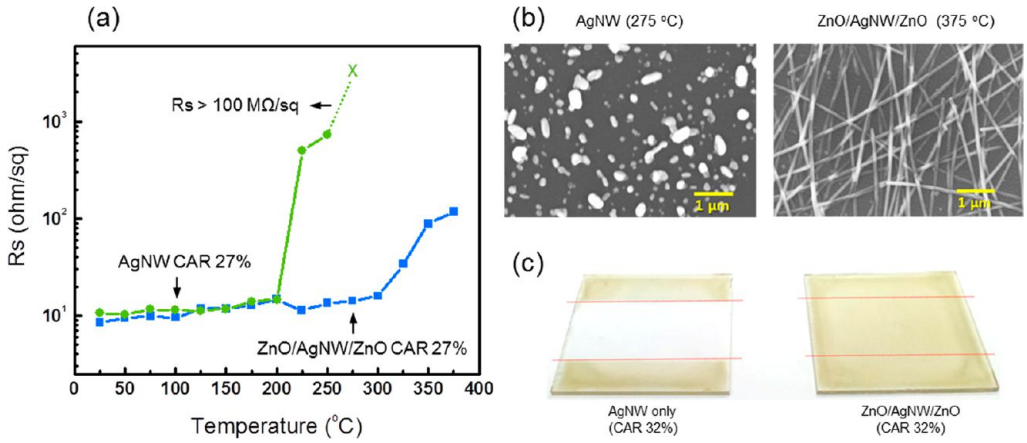

Figure 5. (a) Variations of the resistances of the AgNW single film (CAR = 27%) and the ZnO/AgNW/ZnO composite film (CAR = 27%) on glass substrates as a function of the annealing temperature. (b) SEM images of a AgNW single film and a ZnO/AgNW/ZnO film after thermal stability testing. The AgNW single film was heated to 275 °C, while the ZnO/AgNW/ZnO film was heated to 375 °C. (c) Photographs of the AgNW single film (left) and ZnO/AgNW/ZnO film (right) on glass substrates after the adhesion test. Scotch tape was firmly attached on the electrode surfaces, followed by rapid detachment. To distinguish the difference between the removed and remaining regions, the AgNW films with a higher density (CAR = 32%) were used for the tape test.

additional issues such as thermal instability and poor adhesion properties. We performed a thermal stability test by measuring the sheet resistance as a function of the annealing temperature. In the case of the AgNW single film, a rapid increase of the sheet resistance was observed at 225 °C, and at temperatures above 300 °C, the sheet resistance exceeded the measurement limit (>100 MΩ/sq) (Figure 5a). The SEM image of the AgNW surface after annealing at 275 °C indicates that the rapid increase of the sheet resistance can be attributed to the disconnection of AgNW networks. The AgNWs start to be fragmented, forming chains of isolated droplets upon melting, as shown in Figure 5b (left).[39] This thermal instability can be relieved by constructing the ZnO/AgNW/ZnO composite structure. Ramasamy *et al.* demonstrated the improvement of AgNW thermal properties by atomic layer deposition of TiO_2 around the nanowire surfaces.[40]

Our ZnO/AgNW/ZnO composite electrode did show similar enhancement in which there was no sudden increase of the resistance until 375 °C, despite of the slight increase up to this point (Figure 5a). The composite electrode exhibited a sheet resistance of about 15 Ω/sq at 300 °C, where the AgNW single film completely lost its conductance. As shown in Figure 5b (right), the AgNWs embedded in the layered composite maintained their high aspect ratio morphology without coalescence into isolated droplet-shaped Ag particles when annealed at 375 °C. The SEM backscattered image and HRTEM cross-section images clearly confirmed the improved thermal stability of the composite electrode, as shown in Figure S3 (Supporting Information). Even though some of the nanowires were partially melted and their length became shorter, a percolating network was still maintained while the junctions bulged out due to Ag migration, leaving behind an empty channel made by ZnO. Another important factor related to the device stability and durability is its adhesion property. The AgNW thin film without a protective layer on the substrate is vulnerable to physical damages such as scratches and detachment. In the ZnO/AgNW/ZnO structure, AgNWs were embedded and coated with ZnO layers, which can play a role as a protection layer. Figure 5c shows the results of the adhesion test using 3M scotch tape. In the case of the AgNW single layer, the AgNWs were easily detached from the substrate by the scotch tape, whereas the ZnO/AgNW/ZnO composite film remained intact, indicative of strong adhesion.

Thin film solar cells involving different types of transparent electrodes were fabricated using a CIGSSe absorber layer and a ZnS buffer layer on top of a Mo-coated glass substrate. The schematic structure of thin film solar cells using ITO, a AgNW single film, and the ZnO/AgNW/ZnO electrode is shown in Figure 6a. Except for the top transparent electrode, all layers in the devices were fabricated under identical process conditions. Figure 6b shows the photocurrent density−voltage (J−E) curves of the CIGSSe thin film solar cells based on various top electrodes measured under 100 mW/cm^2 illumination (AM 1.5G condition). The reference thin film solar cell based on the sputtered ITO transparent electrode shows an open circuit voltage (V_{oc}) of 0.432 V, a short circuit current (J_{sc}) of 28.5 mA/cm^2, a fill factor (FF) of 43.2%, and a calculated power conversion efficiency (PCE) of 5.32%. These performance values are relatively lower than the values reported for sputtered CIGSSe thin film solar cells. This discrepancy is present because a ZnS buffer layer was utilized instead of CdS, which is known to outperform ZnS, and the deposit conditions of the absorber and buffer layers were not yet optimized. However, the ZnS/CIGSSe/Mo/glass could serve as a platform to compare the influence of the top transparent electrodes.

Table 2 summarizes the cell performances of thin film solar cells fabricated using different transparent

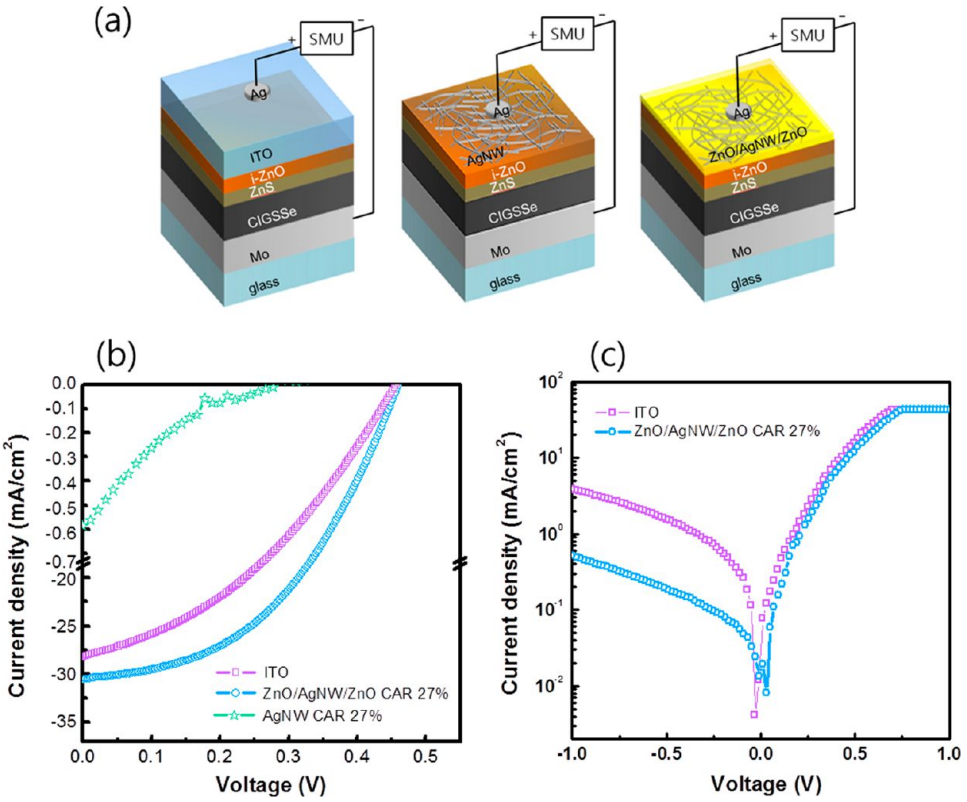

Figure 6. (a) Schematic structures of CIGSSe thin film solar cells using different transparent conductors such as a sputtered ITO single film, a AgNW single film, and a ZnO/AgNW/ZnO composite film. All of the other layers such as the absorber and buffer are identical. (b) Current density–voltage characteristics for the thin film solar cells based on the various top electrodes. (c) Current density–voltage characteristics measured in the dark are also displayed to compare the leakage current between the cells with the ITO and the ZnO/AgNW/ZnO composite.

electrodes. The thin film solar cell based on ZnO double layers without a AgNW layer demonstrated poor performance because of its high resistance. The insertion of a AgNW layer between the ZnO double layers significantly improved the cell performances due to the dramatic decrease of the sheet resistance. The thin film solar cell using the ZnO/AgNW/ZnO (CAR = 27%) exhibited a V_{oc} of 0.458 V, a J_{sc} of 31.0 mA/cm^2, a FF of 45%, and a calculated PCE of 6.37%. Higher J_{sc} and PCE values were observed compared to the reference cell based on the ITO electrode. This can be ascribed to the enhancement of the optical and electrical properties resulting from the synergetic effect of the combination of ZnO and AgNWs. The low sheet resistance makes it possible to effectively transport the charge carriers generated in the solar cell to the front contacts, reducing the current loss at the electrode. In this respect, ITO is generally preferred over ZnO as a window electrode in solar cell devices.

We accomplished a highly conductive ZnO–AgNW composite electrode by inserting a AgNW film between the ZnO layers, as compared to either sputtered ITO or ZnO single films, which resulted in a lower sheet resistance and a higher J_{sc}. In addition, the ZnO overcoat layer assists the charge carrier collection, acting as an efficient electron extraction layer and, in turn, increasing the J_{sc} value, as shown in the ZnO nanoparticle dispersed AgNW network structure, which has shown better charge collection efficiency in solar cell applications.[28] For the solar cell using the AgNW film without ZnO layers, the J_{sc} value was too low in spite of its low sheet resistance (Figure 6b). This observation supports the role of ZnO layers in the composite electrode in which the extension of the effective area for charge collection results in an increased J_{sc}.

TABLE 2. Performance Comparison of Thin Film Solar Cells Fabricated Using Different Transparent Electrodes: ZnO/AgNW/ZnO (CAR = 27%), Sputtered ZnO Double Layer (CAR = 0%), AgNW Single Film (CAR = 27%), and Sputtered ITO Single Electrodes

window electrode type	J_{sc} (mA/cm^2)	V_{oc} (V)	FF	PCE (%)
ITO	28.5	0.432	0.432	5.32
AgNW (CAR = 27%)	0.54	0.280	0.154	0.029
ZnO/ZnO (CAR = 0%)	0.028	0.184	0.245	0.0013
ZnO/AgNW/ZnO (CAR = 27%)	31.0	0.458	0.450	6.37

The *i*-ZnO layer and the ZnO layer in ZnO/AgNW/ZnO composite have different conductivities. The ZnO layer in the composite is more conductive than *i*-ZnO layer. The ZnO film comprising ZnO/AgNW/ZnO multilayer has R_s about 135 950 Ω/sq, while the *i*-ZnO film has too high R_s (>100 M Ω/sq) beyond the measurement

limit. We can assume the generation of the same amount of electrons in thin film solar cells since the two cells have the same cell part (*i*-ZnO/ZnO/CIGSSe/Mo) and the top electrodes have similar transmittances (T of AgNW film = 90.81% and T of ZnO/AgNW/ZnO = 91.91%). If such, the J_{sc} would be determined by the number of electrons collected by the top electrode. For the AgNW top electrode, it is possible to collect only the electrons located near the direct contact between AgNW and the *i*-ZnO layer. The AgNW film has a large open area between nanowire networks, thus the effective charge collection area is very limited. On the other hand, in the ZnO/AgNW/ZnO top electrode, a relatively conductive ZnO layer can transport more electrons to AgNWs even from the regions far away from AgNW locations, as illustrated in Figure S4 (Supporting Information).

The enlarged effective charge collection area makes the solar cell with ZnO/AgNW/ZnO/*i*-ZnO exhibit a higher J_{sc} than the one with the AgNW/*i*-ZnO cell. The V_{oc} values were also improved when using the ZnO/AgNW/ZnO composite electrode. The lower V_{oc} associated with the reference ITO-based solar cells is likely related to the leakage current through the cell due to its low resistivity. The current density−voltage data were measured in the dark, as shown in Figure 6c. The current flowing at the negative voltage region in the dark represents the leakage current across the cells. The leakage current of the ZnO/AgNW/ZnO incorporated cell was 8 times lower than that of the ITO-based cell. Sandwiching the highly conductive metallic network with relatively resistive ZnO thin films can reduce the leakage current.

The higher transmittance of our composite electrodes explains the higher PCE compared to the reference ITO-based solar cells since more light is transmitted to the absorber layer, generating more charge carriers. To gain in-depth understanding of the influence of the optical properties of the electrodes on the cell performances, we measured the external quantum efficiency (EQE) of the CIGSSe cells with different transparent electrodes. Since the identical absorber/buffer layers were used, we can assume that the internal quantum efficiency (IQE) is the same for all of the samples. In such a case, the EQE is indicative of the influence of a transparent electrode. Two devices showed rather efficient photoconversion efficiencies at wavelengths in the range of 440−960 nm, while the EQE values were 50−70%, as shown in Figure 7a. For the cell with the ZnO/AgNW/ZnO (CAR = 27%) composite electrode, the highest EQE value of 70.3% at 600 nm was obtained. This efficiency is superior to the highest EQE value of 65% at 560 nm for the reference cell with an ITO film.

To compare the EQE values between the composite electrode and the ITO electrode-based cells, the relative change of the EQE values is displayed in Figure 7b. Here, $\Delta EQE/EQE(\lambda)$ is defined as $(EQE_{ZnO/AgNW/ZnO}(\lambda) - EQE_{ITO\text{-}only}(\lambda))/EQE_{ITO\text{-}only}(\lambda)$, where $EQE_{ZnO/AgNW/ZnO}(\lambda)$ and $EQE_{ITO\text{-}only}(\lambda)$ are the EQE values at a wavelength of λ for the CIGSSe cell with ZnO/AgNW/ZnO and only ITO, respectively. ΔEQE has a positive value and increases above 440 nm, indicating that the cell with ZnO/AgNW/ZnO shows a higher quantum efficiency than the cell with ITO at wavelengths above 440 nm and that the EQE improvement is significant at relatively longer wavelengths. This can be supported by the observed differences in the optical properties between the ZnO/AgNW/ZnO composite electrode and the ITO electrode. Figure 7c shows the relative change of the reflectance values (R%) using the data presented in Figure 2d. $\Delta R\%/R\%(\lambda)$ is defined as $(R\%_{ZnO/AgNW/ZnO}(\lambda) - R\%_{ITO\text{-}only}(\lambda))/R\%_{ITO\text{-}only}(\lambda)$, where $R\%_{ZnO/AgNW/ZnO}(\lambda)$ and $R\%_{ITO\text{-}only}(\lambda)$ are the R% values at a wavelength of λ for ZnO/AgNW/ZnO on glass and ITO on glass, respectively. A reduction of the R% value was observed in the visible light region at wavelengths of about 460−750 nm, suggesting that the composite

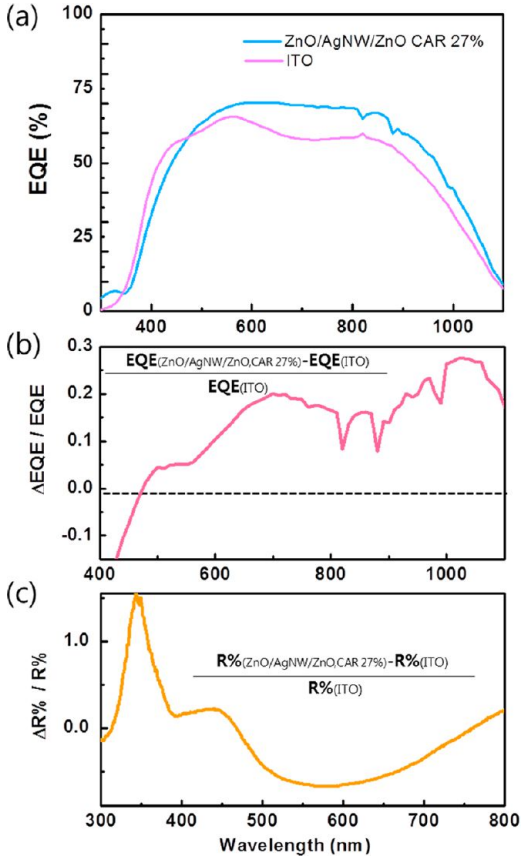

Figure 7. (a) External quantum efficiency (EQE) spectra of an ITO single film and ZnO/AgNW/ZnO composite electrode incorporated CIGSSe thin film solar cells. (b) Relative change of the EQE, $\Delta EQE/EQE(\lambda) = (EQE_{ZnO/AgNW/ZnO}(\lambda) - EQE_{ITO\text{-}only}(\lambda))/EQE_{ITO\text{-}only}(\lambda)$, where $EQE_{ZnO/AgNW/ZnO}(\lambda)$ and $EQE_{ITO\text{-}only}(\lambda)$ are the EQE values a wavelength of λ for the ZnO/AgNW/ZnO-based CIGSSe thin solar cell and ITO-only CIGSSe cell, respectively. (c) Relative change of the reflectance (R), $\Delta R\%/R\%(\lambda) = (R\%_{ZnO/AgNW/ZnO}(\lambda) - R\%_{ITO\text{-}only}(\lambda))/R\%_{ITO\text{-}only}(\lambda)$, where $R\%_{ZnO/AgNW/ZnO}(\lambda)$ and $R\%_{ITO\text{-}only}(\lambda)$ are the R% values at a wavelength of λ for ZnO/AgNW/ZnO on glass and ITO on glass, respectively.

electrode has a lower reflectance than the ITO film in the visible light region due to the anti-reflection effect of the AgNW layer. The light trapping effect may also be possible because of the enhanced light scattering by AgNWs.[41] This means that the composite electrode passes incident sun light to the absorber layer more effectively, enhancing the EQE values.

CONCLUSIONS AND PROSPECTS

We proposed a ZnO/AgNW/ZnO multilayer as a novel transparent composite electrode which demonstrated good thermal and mechanical stabilities as well as a high conductivity and good transparency. By inserting a AgNW network layer between ZnO layers, the sheet resistance was dramatically decreased without sacrificing the transparency. The AgNW density in the ZnO/AgNW/ZnO composite plays an important role in determining the figure of merit, which was maximized at a CAR value of 27%. Our ZnO/AgNW/ZnO composite electrode showed a higher tolerance to bending stress than the conventional ITO film as well as good thermal stability and strong adhesiveness, which the AgNW single film lacked. The improved thermal and mechanical stabilities as well as the high value of figure of merit are attributed to the unique structure of the layered composite. The ZnO layer conformally covers the AgNWs filling the empty area and tightening the AgNW junctions, and it may act as an encapsulate that protects the nanowires from oxidation/melting, improving the mechanical and thermal stabilities of the embedded AgNW film. Our ZnO/AgNW/ZnO composite also serves well as an effective window electrode for Cu chalcogenide thin film solar cells. The CIGSSe thin film solar cells based on the ZnO/AgNW/ZnO electrode showed 20% higher PCE and EQE performances than the cell using the conventional sputtered ITO electrode. The AgNW layer inserted between the ZnO allows more effective light transmission at the visible wavelengths due to the reduced specular reflectance, while maintaining a high electrical conductance. In addition, the ZnO overcoat layer that fills the empty spaces between the AgNWs would assist the charge carrier collection and, at the same time, reduce the leakage current, which results in higher J_{sc}, PCE%, and EQE values. All of these findings clearly demonstrate that our indium-free ZnO/AgNW/ZnO composite may become a robust, flexible, cost-effective, high-performance transparent electrode that enables higher power conversion efficiency in thin film solar cells.

METHODS AND MATERIALS

ZnO/AgNW/ZnO Electrode Fabrication. ZnO/AgNW/ZnO multilayer electrodes were prepared by direct current (dc) magnetron sputtering at room temperature with various AgNW densities. The bottom ZnO layer with a thickness of 33 nm was sputtered using a ZnO target at a constant dc power of 150 W, an Ar flow of 50 cc, and a working pressure of 5 mTorr on a glass substrate (20×20 mm^2). After the sputtering of the bottom ZnO layer, a AgNW layer with various densities was deposited by spin coating on the ZnO layer from a AgNW dispersion (Cambrios Technologies Corp.). AgNW films were dried at 50 °C for 90 s and 140 °C for 90 s. Then, UV treatment was performed to remove organic contaminants prior to the top layer deposition. Finally, an additional ZnO layer with a thickness of 33 nm was deposited on the AgNW layer under the same sputtering conditions.

Optical and Structural Characterization. The optical transmittance and reflectance of the ZnO/AgNW/ZnO composite electrode were measured at room temperature using a UV−vis spectrophotometer (Cary 100, Agilent Technologies) equipped with an integrating sphere (DRA-CA-30I, Labsphere) in the wavelength range from 300 to 900 nm. All recorded transmittance spectra were normalized with respect to a glass substrate, and reflectance spectra were taken using a certified reflectance standard (Labsphere) as the zero absorbance reference after baseline subtraction and normalization. The surface morphology of the AgNWs obtained under different rotation speeds on the bottom ZnO layer and ZnO/AgNW/ZnO composite electrode was analyzed by a scanning electron microscope (SEM, JSM-6010LV, JEOL Ltd.) at an operating voltage of 15 kV and atomic force microscopy (AFM, SPA 400, SEIKO). The compositional contrast was also revealed by SEM backscattering electron imaging. The cross section of the ZnO/AgNW/ZnO composite was analyzed by a high-resolution transmission electrode microscope (HRTEM, JEM-2100F, JEOL Ltd.). Samples for TEM analysis were prepared using a FEI Nova 600 DB-FIB.

Electrical, Mechanical, and Thermal Stability Measurements. The sheet resistances of the ZnO/AgNW/ZnO samples were measured by a four-point probe system (RS8, BEGA Technologies) as a function of the CAR value. The resistance reported here is the average value obtained after at least five multiple measurements. The mechanical stabilities of the ZnO/AgNW/ZnO composites and ITO film as a function of the number of bend cycles were determined by repeatedly bending the composite films with a two-point bending device consisting of two parallel plates, where the radius of curvature was set at 3 mm and the bend speed was about one cycle per second. The sheet resistance values were measured on the flattened film after the given bending cycles by a four-point probe. Thermal stability testing was also performed by monitoring the change of the sheet resistance of the ZnO/AgNW/ZnO composite and the AgNW film with the same CAR as a function of the annealing temperature. 3M scotch tape was used for adhesion testing of the ZnO/AgNW/ZnO composite film and AgNW film on the glass substrate. 3M scotch tape was applied on the film surface after removing all entrapped air, and the time between the application and removal of the tape was less than 1 min. The tape was removed by a rapid pull force applied perpendicular to the test area.

Thin Film Solar Cell Fabrication. We prepared CIGSSe thin film solar cells to compare the influences of the different transparent top electrodes. Identical sputtered CIGSSe absorber and chemical bath-deposited ZnS buffer layers were used for all of the samples. Intrinsic (*i*) ZnO layers with a thickness of 50 nm were deposited by dc sputtering at a constant dc power of 150 W at 100 °C, a gas flow ratio of Ar/O_2 = 50 cc/5 cc under a working pressure of 5 mTorr. After the deposition of the *i*-ZnO layer, the ZnO/AgNW/ZnO transparent composite electrodes were fabricated as described above. For the reference sample, an ITO single layer with a thickness of 500 nm was prepared by radio frequency (RF) magnetron sputtering (RF power of 200 W at 100 °C, Ar flow rate of 50 cc, and a working pressure of 5 mTorr). The solar cell containing only AgNWs as a transparent electrode was also fabricated by spin coating the AgNW dispersion on the *i*-ZnO/ZnS/CIGSSe/Mo substrate. Finally, the silver front contacts were made on the window electrodes as a dot shape (diameter = 1 mm) by silver paste.

Characterization of the Thin Film Solar Cells. The solar cells were characterized by measuring the photocurrent density−voltage ($J-V$) curves and external quantum efficiency (EQE). The photovoltaic performance in terms of the $J-V$ of the devices was determined by means of a solar simulator (Sol3A Class AAA, Oriel Instruments) and a Keithley 2400 source measurement unit, whereas the EQE was obtained by a quantum efficiency measurement system (QEX10, PV Measurements, Inc.) carried out under air mass (AM) 1.5 and 1 sun (100 mW/cm^2) conditions. The 1 sun intensity level was calibrated using a standard Si reference cell certified by Newport Corporation. From the measured J_{sc}, V_{oc}, and FF values, PCE values were calculated by applying PCE = FF × V_{oc} × J_{sc}/P_s, where P_s is the input solar irradiance (mW/cm^2). The FF is defined as FF = $J_mV_m/J_{sc}V_{oc}$, where J_m and V_m are the maximum current and voltage, respectively.

Conflict of Interest: The authors declare no competing financial interest.

Acknowledgment. This work was supported by the National Research Foundation of Korea (NRF) grant funded by the Korea government (MEST) (No. 2012R1A3A2026417). It was also partially supported by the Second Stage of the Brain Korea 21 Project.

Supporting Information Available: Topography images of the AgNW single film and ZnO/AgNW/ZnO composite film obtained by atomic force microscopy (AFM). Transmittance and sheet resistance of the AgNW single film depending on the function of the CAR%. The SEM backscattered image and HRTEM images of the ZnO/AgNW/ZnO composite electrode before and after thermal stability testing. This material is available free of charge *via* the Internet at http://pubs.acs.org.

REFERENCES AND NOTES

1. Gordon, R. G. Criteria for Choosing Transparent Conductors. *MRS Bull.* **2000**, *25*, 52–57.
2. Müller, J.; Rech, B.; Springer, J.; Vanecek, M. TCO and Light Trapping in Silicon Thin Film Solar Cells. *Sol. Energy* **2004**, *77*, 917–930.
3. Lee, J.-Y.; Connor, S. T.; Cui, Y.; Peumans, P. Semitransparent Organic Photovoltaic Cells with Laminated Top Electrode. *Nano Lett.* **2010**, *10*, 1276–1279.
4. Lee, J.-Y.; Connor, S. T.; Cui, Y.; Peumans, P. Solution-Processed Metal Nanowire Mesh Transparent Electrodes. *Nano Lett.* **2008**, *8*, 689–692.
5. Hu, L.; Kim, H. S.; Lee, J.-Y.; Peumans, P.; Cui, Y. Scalable Coating and Properties of Transparent, Flexible, Silver Nanowire Electrodes. *ACS Nano* **2010**, *4*, 2955–2963.
6. Leem, D.-S.; Edwards, A.; Faist, M.; Nelson, J.; Bradley, D. D. C.; Mello, J. C. Efficient Organic Solar Cells with Solution-Processed Silver Nanowire Electrodes. *Adv. Mater.* **2011**, *23*, 4371–4375.
7. Scardaci, V.; Coull, R.; Lyons, P. E.; Rickard, D.; Coleman, J. N. Spray Deposition of Highly Transparent, Low-Resistance Networks of Silver Nanowires over Large Areas. *Small* **2011**, *7*, 2621–2628.
8. Bergin, S. M.; Chen, Y.-H.; Rathmell, A. R.; Charbonneau, P.; Li, Z.-Y.; Wiley, B. J. The Effect of Nanowire Length and Diameter on the Properties of Transparent, Conducting Nanowire Films. *Nanoscale* **2012**, *4*, 1996–2004.
9. De, S.; Higgins, T. M.; Lyons, P. E.; Doherty, E. M.; Nirmalraj, P. N.; Blau, W. J.; Boland, J. J.; Coleman, J. N. Silver Nanowire Networks as Flexible, Transparent, Conducting Films: Extremely High DC to Optical Conductivity Ratios. *ACS Nano* **2009**, *3*, 1767–1774.
10. Rathmell, A. R.; Bergin, S. M.; Hua, Y.-L.; Li, Z.-Y.; Wiley, B. J. The Growth Mechanism of Copper Nanowires and Their Properties in Flexible, Transparent Conducting Films. *Adv. Mater.* **2010**, *22*, 3558–3563.
11. Madaria, A. R.; Kumar, A.; Ishikawa, F. N.; Zhou, C. Uniform, Highly Conductive, and Patterned Transparent Films of a Percolating Silver Nanowire Network on Rigid and Flexible Substrate Using a Dry Transfer Technique. *Nano Res.* **2010**, *3*, 564–573.
12. Kim, Y. H.; Sachse, C.; Machala, M. L.; May, C.; Müller-Meskamp, L.; Leo, K. Highly Conductive PEDOT:PSS Electrode with Optimized Solvent and Thermal Post-treatment for ITO-Free Organic Solar Cells. *Adv. Funct. Mater.* **2011**, *21*, 1076–1081.
13. Na, S.-I.; Kim, S.-S.; Jo, J.; Kim, D.-Y. Efficient and Flexible ITO-Free Organic Solar Cells Using Highly Conductive Polymer Anodes. *Adv. Mater.* **2008**, *20*, 4061–4067.
14. Wu, Z.; Chen, Z.; Du, X.; Logan, J. M.; Sippel, J.; Nikolou, M.; Kamaras, K.; Reynolds, J. R.; Tanner, D. B.; Hebard, A. F.; *et al.* Transparent, Conductive Carbon Nanotube Films. *Science* **2004**, *305*, 273–1276.
15. Contreras, M. A.; Barnes, T.; Lagemaat, J. V. D.; Rumbles, G.; Coutts, T. J.; Weeks, C.; Glatkowski, P.; Levitsky, I.; Peltola, J.; Britz, D. A. Replacement of Transparent Conductive Oxides by Single-Wall Carbon Nanotubes in Cu(In,Ga)Se_2-Based Solar Cells. *J. Phys. Chem. C* **2007**, *111*, 14045–14048.
16. Rowell, M. W.; Topinka, M. A.; McGehee, M. D.; Prall, H.-J.; Dennler, G.; Sariciftci, N. S.; Hu, L.; Gruner, G. Organic Solar Cells with Carbon Nanotube Network Electrodes. *Appl. Phys. Lett.* **2006**, *88*, 233506.
17. Wang, X.; Zhi, L.; Mullen, K. Transparent, Conductive Graphene Electrodes for Dye-Sensitized Solar Cells. *Nano Lett.* **2008**, *8*, 323–327.
18. Becerril, H. A.; Mao, J.; Liu, Z.; Stoltenberg, R. M.; Bao, Z.; Chen, Y. Evaluation of Solution-Processed Reduced Graphene Oxide Films as Transparent Conductors. *ACS Nano* **2008**, *2*, 463–470.
19. Jo, G.; Na, S.-I.; Oh, S.-H.; Lee, S.; Kim, T.-S.; Wang, G.; Choe, M.; Park, W.; Yoon, J.; Kim, D.-Y.; *et al.* Tuning of a Graphene-Electrode Work Function To Enhance the Efficiency of Organic Bulk Heterojunction Photovoltaic Cells with an Inverted Structure. *Appl. Phys. Lett.* **2010**, *97*, 213301.
20. Ihn, S.-G.; Shin, K.-S.; Jin, M.-J.; Bulliard, X.; Yun, S.; Choi, Y. S.; Kim, Y.; Park, J.-H.; Sim, M.; Kim, M.; *et al.* ITO-Free Inverted Polymer Solar Cells Using a GZO Cathode Modified by ZnO. *Sol. Energy Mater. Sol. Cells* **2011**, *95*, 1610–1614.
21. Sio, A. D.; Chakanga, K.; Sergeev, O.; Maydell, K. V.; Parisi, J.; Hauff, E. V. ITO-Free Inverted Polymer Solar Cells with ZnO: Al Cathodes and Stable Top Anodes. *Sol. Energy Mater. Sol. Cells* **2012**, *98*, 52–56.
22. Nunesa, P.; Fortunatoa, E.; Tonelloa, P.; Braz Fernandesa, F.; Vilarinhob, P.; Martins, R. Effect of Different Dopant Elements on the Properties of ZnO Thin Films. *Vacuum* **2002**, *64*, 281–285.
23. Lu, Y. C.; Chou, K. S. Tailoring of Silver Wires and Their Performance as Transparent Conductive Coatings. *Nanotechnology* **2010**, *21*, 215707.
24. Gaynor, W.; Burkhard, G. F.; McGehee, M. D.; Peumans, P. Smooth Nanowire/Polymer Composite Transparent Electrodes. *Adv. Mater.* **2011**, *23*, 2905–2910.
25. Sahu, D. R.; Lin, S.-Y.; Huang, J.-L. ZnO/Ag/ZnO Multilayer Films for the Application of a Very Low Resistance Transparent Electrode. *Appl. Surf. Sci.* **2006**, *252*, 7509–7514.
26. Kao, K.-S.; Chang, S.-H.; Hsieh, P.-T.; Wang, C.-M.; Cheng, D.-L. Transparence and Electrical Properties of ZnO-Based Multilayer Electrode. *Appl. Phys. A: Mater. Sci. Process.* **2009**, *96*, 529–533.
27. Sahu, D. R.; Huang, J.-L. High Quality Transparent Conductive ZnO/Ag/ZnO Multilayer Films Deposited at Room Temperature. *Thin Solid Films* **2006**, *515*, 876–879.
28. Han, H.; Theodore, N. D.; Alford, T. L. Improved Conductivity and Mechanism of Carrier Transport in Zinc Oxide with Embedded Silver Layer. *J. Appl. Phys.* **2008**, *103*, 013708.
29. Jeong, J.-A.; Kim, J. H.; Kim, H.-K. Ag Grid/ITO Hybrid Transparent Electrodes Prepared by Inkjet Printing. *Sol. Energy Mater. Sol. Cells* **2011**, *95*, 1974–1978.
30. Stubhan, T.; Krantz, J.; Li, N.; Guo, F.; Litzov, I.; Steidl, M.; Richter, M.; Matt, G. J.; Brabec, C. J. High Fill Factor Polymer Solar Cells Comprising a Transparent, Low Temperature Solution Processed Doped Metal Oxide/Metal Nanowire Composite Electrode. *Sol. Energy Mater. Sol. Cells* **2012**, *107*, 248–251.
31. Fan, J. C. C.; Bachner, F. J.; Foley, G. H.; Zavracky, P. M. Transparent Heat-Mirror Films of TiO_2/Ag/TiO_2 for Solar Energy Collection and Radiation Insulation. *Appl. Phys. Lett.* **1974**, *25*, 693–695.

32. Chopra, K. L.; Paulson, P. D.; Dutta, V. Thin-Film Solar Cells: An Overview. *Prog. Photovoltaics* **2004**, *12*, 69–92.
33. Haacke, G. New Figure of Merit for Transparent Conductors. *J. Appl. Phys.* **1976**, *47*, 4086–4089.
34. Ajuria, J.; Ugarte, I.; Cambarau, W.; Etxebarria, I.; Tena-Zaera, R.; Pacios, R. Insights on the Working Principles of Flexible and Efficient ITO-Free Organic Solar Cells Based on Solution Processed Ag Nanowire Electrodes. *Sol. Energy Mater. Sol. Cells* **2012**, *102*, 148–152.
35. Liu, C.-H.; Yu, X. Silver Nanowire-Based Transparent, Flexible, and Conductive Thin Film. *Nanoscale Res. Lett.* **2011**, *6*, 75.
36. Hsu, P.-C.; Wu, H.; Carney, T. J.; McDowell, M. T.; Yang, Y.; Garnett, E. C.; Li, M.; Hu, L.; Cui, Y. Passivation Coating on Electrospun Copper Nanofibers for Stable Transparent Electrodes. *ACS Nano* **2012**, *6*, 5150–5156.
37. Morgenstern, F. S. F.; Kabra, D.; Massip, S.; Brenner, T. J. K.; Lyons, P. E; Coleman, J. N.; Friend, R. H. Ag-Nanowire Films Coated with ZnO Nanoparticles as a Transparent Electrode for Solar Cells. *Appl. Phys. Lett.* **2011**, *99*, 183307.
38. Alzoubi, K.; Hamasha, M. M.; Lu, S.; Sammakia, B. Bending Fatigue Study of Sputtered ITO on Flexible Substrate. *J. Disp. Technol.* **2011**, *7*, 593–600.
39. Toimil Molares, M. E.; Balogh, A. G.; Cornelius, T. W.; Neumann, R.; Trautmann, C. Fragmentation of Nanowires Driven by Rayleigh Instability. *Appl. Phys. Lett.* **2004**, *85*, 5337–5339.
40. Ramasamy, P.; Seo, D.-M.; Kim, S.-H.; Kim, J. W. Effects of TiO_2 Shells on Optical and Thermal Properties of Silver Nanowires. *J. Mater. Chem.* **2012**, *22*, 11651–11657.
41. Groep, J.; Spinelli, P.; Polman, A. Transparent Conducting Silver Nanowire Networks. *Nano Lett.* **2012**, *12*, 3138–3144.